RAD Conference Proceedings, vol. 6, pp. 26–30, 2022
ISSN 2466-4626 (online) | DOI: 10.21175/RadProc.2022.05
www.rad-proceedings.org

EXPERIMENTAL MEASUREMENT OF SECONDARY NEUTRONS ON PARTICLE ACCELERATORS

Aleš Jančář[1*], Zdeněk Kopecký[1], Jiří Čuleň[1], Filip Mravec[1], Zdeněk Matěj[2]

[1]VF, a.s., Černá Hora, Czech Republic
[2]Masaryk University, Brno, Czech Republic

Abstract. *A newly developed fast digital spectrometer for neutron spectroscopy is presented. The pulse shape discrimination (PSD) performance of the spectrometer has been evaluated within two experiments with different neutron energies. The experimental measurements of secondary neutrons were carried out in the laboratory of the Van de Graaff accelerator and at the Proton Therapy Center in Prague. For both experiments, a liquid scintillator detector BC-501A (NE-213) was used. The results of experiments demonstrate the very good quality of the PSD discrimination of the spectrometer. The experimental spectra of secondary neutrons were compared with spectra obtained by means Monte Carlo simulations. The detector response matrix and the flux of secondary neutrons and protons in the vicinity of irradiated proton therapy phantom were calculated using Monte Carlo simulations.*

Keywords: *scintillation detectors, mono-energetic neutron sources, pulse-shape discrimination, ADC, FPGA, digital-signal processing*

1. INTRODUCTION

The interaction of the primary proton beam in proton accelerators is the source of secondary neutrons and many other secondary particles. For scientific applications, fast neutrons can be generated at Van de Graaff accelerators. In proton therapy, the high-energy proton beam causes the production of secondary neutrons. This subsequently leads to an unwanted dose contribution.

Technology advancements in the field of digital electronics make it possible to design very fast and high-quality neutron spectrometers with great application potential. By applying the PSD method, the spectrometers allow distinguishing between neutron and photon pulses in real-time.

This paper presents the results of the measurement of secondary neutrons at the Van de Graaff (VdG) laboratory and Proton therapy center (PTC) in Prague. A cylindrical liquid scintillator detector BC-501A with 12.7 cm diameter and 5.08 cm thickness, purchased from Luxium Solutions, has been connected to a newly developed neutron gamma analyzer NGA-01 (Figure 1) to characterize the secondary neutron field.

2. NEUTRON GAMMA ANALYZER

The neutron gamma analyzer is built as a modular system allowing the use of different types of scintillation detectors. The preamplifier splits the signal from the detector into two branches. Each branch is amplified differently and digitized by a separate ADC. Different amplification increases the dynamic range of particles that the NGA-01 is able to process [1].

Figure 1. Neutron gamma analyzer NGA-01.

The input analog signal from the detector was digitized by two fast ADC converters working with a sampling frequency of 500 MHz. Digital signal processing is implemented into FPGA. The schema of the analyzer is shown in Figure 3.

Measured data from the detector are processed into gamma and neutron spectra. The analyzer NGA-01 is connected to a computer via an optical ethernet of 10 Gbit. The analyzer software is shown in Figure 2.

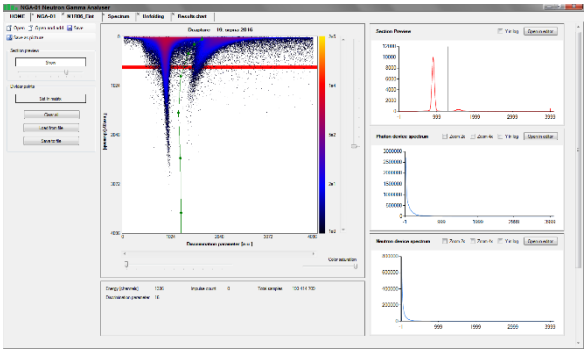

Figure 2. Neutron gamma analyzer software.

* ales.jancar@vfnuclear.com

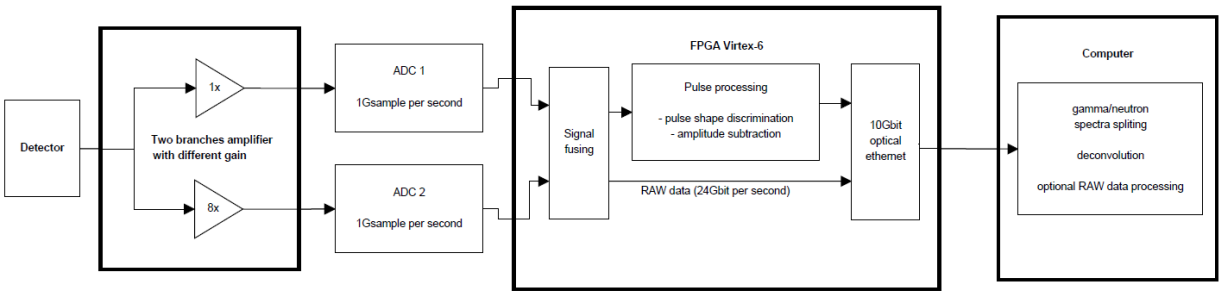

Figure 3. Scheme of neutron gamma analyzer.

3. Pulse-shape discrimination method

The digital spectrometer has incorporated the integration method [2] for recognition of neutron and photon pulses within the signal processing unit. The method is based on pulse charge comparison. The PSD parameter is calculated to recognize neutron and photon events:

$$PSD = \frac{\int_{T_{tail}}^{T_{end}} pulse(t)dt}{\int_{0}^{T_{end}} pulse(t)dt}, \qquad (1)$$

where T_{tail} is an optimized beginning of the tail part of the pulse and T_{end} is an optimized end point of the pulse, see Figure 4.

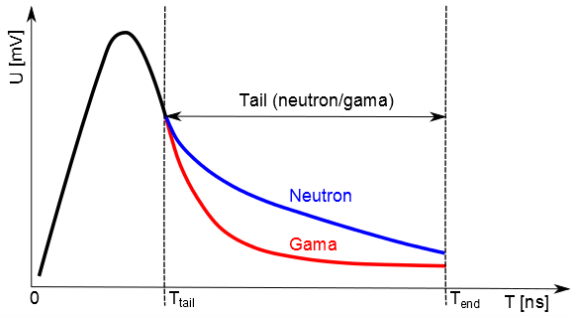

Figure 4. Pulse-shape discrimination by charge integration.

The quality of neutron–gamma discrimination for a given scintillator can be characterized by the figure of merit (FOM) [3, 4]

$$FOM = \frac{\Delta_{gn}}{FHWM_{gamma} + FWHM_{neutron}}, \qquad (2)$$

where Δ_{gn} is the separation between the gamma-ray and neutron peaks and FWHM is the full-width at half maximum of the relevant peak on the corresponding section of the PSD histogram, i.e., the two-dimensional histogram of the light output vs. the PSD parameter. The FOM value greater than 1 is required for an acceptable resolution of neutron and gamma events in the detector. The calculation of FOM is a part of the spectrometer software.

4. Experimental setup

The first measurement was carried out in the Van de Graaff accelerator laboratory of the Institute of Experimental and Applied Physics at the Czech Technical University in Prague. The facility provides well-defined mono-energetic fast neutrons of tunable energy.

The experimental arrangement in the Van de Graaf laboratory is shown in Figure 5. We utilized the experimental channel L1 with a 5 mm beam diameter terminated by a tritium target with a diameter of 40 mm. The accelerating voltage of 1.2 MV and 1μA current was set on the VdG. The incident accelerated deuterons with an energy of 1.2 MeV produced mono-energetic fast neutrons by the 3H(d, n)4He reaction with the maximum kinetic energy of 17.1 MeV along the direction of the experimental deuteron beam channel.

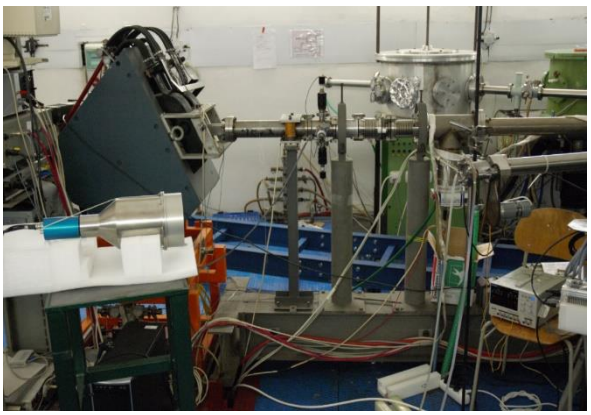

Figure 5. Detector arrangement in the axis of experimental channel in the Van de Graaff accelerator laboratory.

The second measurement was performed at the Proton therapy center in Prague. We used a proton beam that is based on the use of positively charged elementary particles of hydrogen atom nuclei. The protons are accelerated in a Proteus 235 cyclotron type to a speed equal to approximately half the speed of light. This also determines their energy, which reaches up to 230 MeV.

The experimental arrangement in the irradiation room of the Proton Therapy Center is shown in Figure 6. We utilized narrow proton beam with a diameter of 10 mm that was directed into the plastic cylindrical

phantom with a diameter of 250 mm and a height of 310 mm. The distance between the plastic phantom and detector was 1 m. Accelerated protons with energies of 150 and 200 MeV were used. Secondary neutrons were produced by non-elastic reactions with the plastic phantom.

Figure 6. Phantom arrangement in the Proton therapy center.

5. Neutron spectra analysis

The neutron gamma analyzer NGA-01 and the liquid scintillator detector BC-501A have been used for the measurement of the two-parametric PSD spectra. These spectra have been evaluated using newly developed spectrometric software.

Integrated digitized pulses were linearly calibrated in keVee units or keV electron equivalent. The linear transformation coefficients have been derived from positions of the Compton edge [5] in spectra of two gamma-ray sources ^{137}Cs and ^{60}Co. The measurement time was determined according to count rates from the detector. The high voltage on the detector was set to 1.5 kV.

The Compton edge of neutron spectrum with the neutron energy of 17.1 MeV measured in the Van de Graff accelerator laboratory has been utilized for the energy calibration. This calibration was used for the measurement in the Proton therapy center. The deposition energy corresponding to the recoil-proton edge was converted to the electron-equivalent unit using the equation

$$L_p = 0.81E_p - 2.8\left(1-\exp\left(-0.2E_p\right)\right), \quad (3)$$

where E_p and L_p are proton energy and the corresponding electron-equivalent, respectively [6].

6. MCNP simulation

Monte Carlo (MC) simulations of the detector neutron response matrix were performed using the code MCNP 6.2 [7, 8]. The pulse height (PH) spectra for secondary neutrons emitted from the cylindrical phantom during the proton therapy experiment were calculated and compared with the experimental spectra. The simulation utilized particle event tracking in the parallel mode to recognize the PH contributions from different types of particles.

7. Results

The PSD spectrum from a measurement with an incident neutron energy of 17.1 MeV carried out at the VdG laboratory is shown in Figure 7. The PSD resolution of the liquid scintillator has been evaluated and the resulting FOM is presented in Figure 8. The FOM value is greater than 1 over the entire measurement range from 150 keVee.

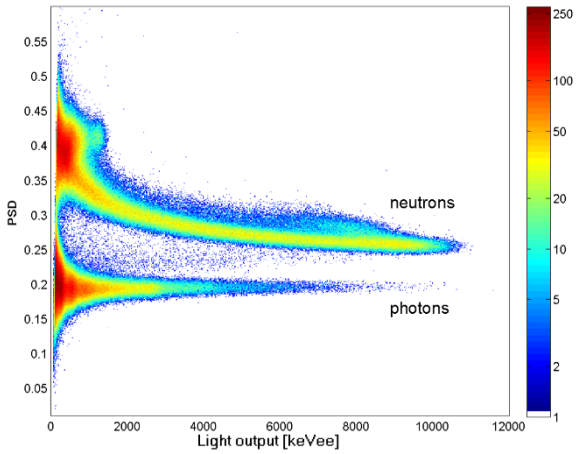

Figure 7. PSD vs. total light 2D plot for the energy of 17.1 MeV.

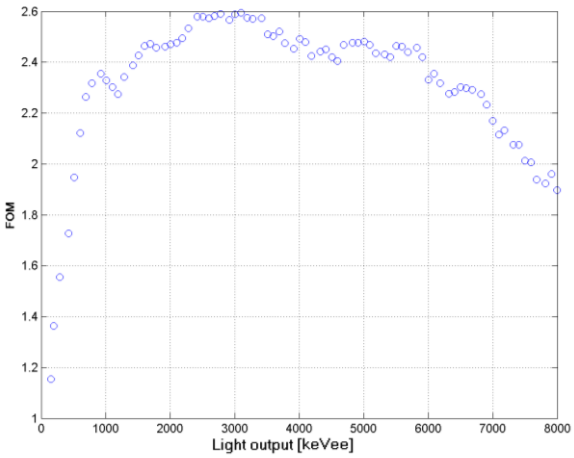

Figure 8. FOM vs. total light for the primary neutron energy of 17.1 MeV.

Proton therapy center measurements with incident proton energies of 150 and 200 MeV are depicted in Figure 9 and Figure 10, respectively. The electron and escaping proton events are separated by the red dashed line from the full-detected proton, deuteron and alpha events.

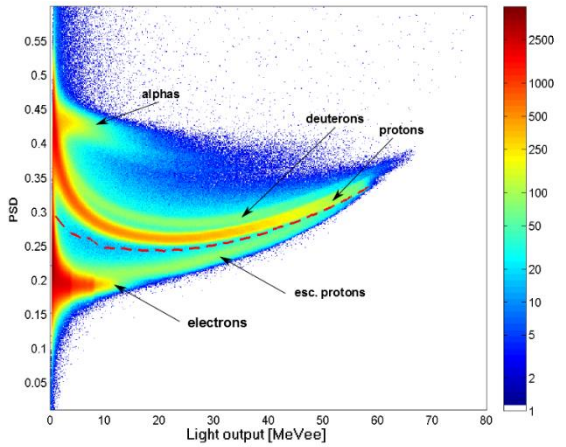

Figure 9. PSD vs. total light 2D plot for primary proton energy of 150 MeV.

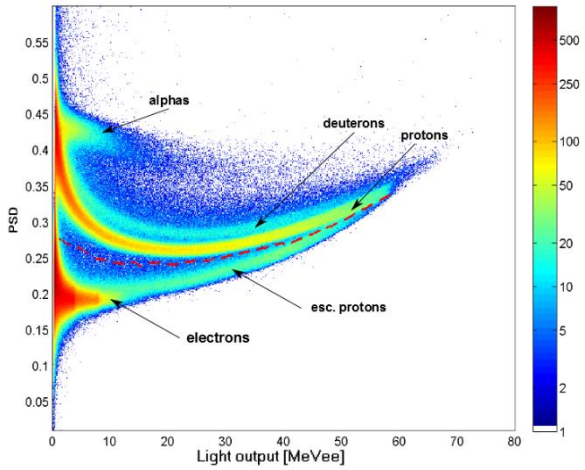

Figure 10. PSD vs. total light 2D plot for primary proton energy of 200 MeV.

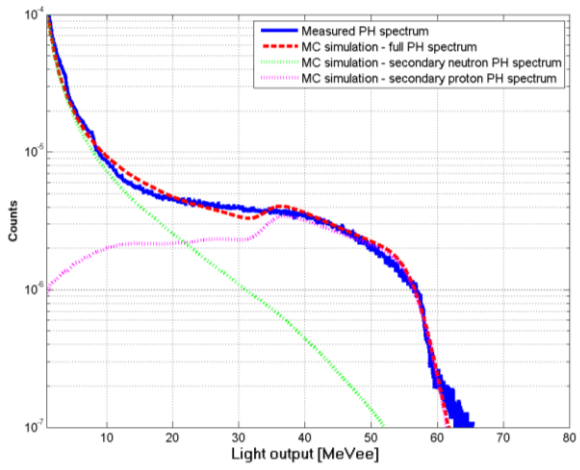

Figure 11. Normalized PH spectrum without photon and escaping proton events for primary proton energy of 150 MeV. PH spectra of incident secondary neutrons and protons are identified using MC simulation.

The PH spectra with excluded electron and escaping proton events are present for incident proton energies of 150 and 200 MeV in Figure 11 and Figure 12, respectively. The PH spectra were created by projecting the PSD diagram according to the red dashed line. The PH spectra were also simulated using the MCNP and the results are in good agreement with the corresponding measured spectra as can be seen in Figure 11 and Figure 12. Within the simulations, the contributions from secondary neutrons and protons generated by the interaction of the incident proton with the phantom were calculated and depicted in Figure 11 and Figure 12.

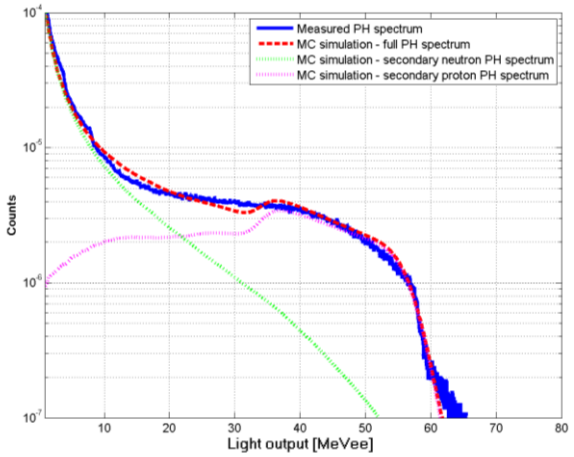

Figure 12. Normalized PH spectrum without photon and escaping proton events for primary proton energy of 200 MeV. PH spectra of incident secondary neutrons and protons are identified using MC simulation.

Using the evaluated MCNP model, we subsequently calculated the detector light output for neutron energies of 10 - 200 MeV (Figure 13) and the spectra of secondary neutrons and protons for incident proton energies of 150 MeV and 200 MeV (Figure 14).

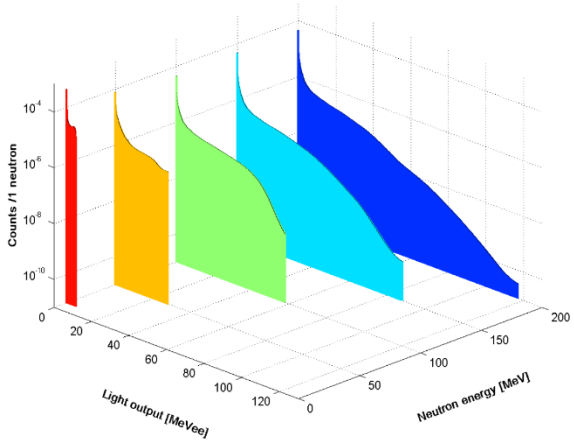

Figure 13. Detector light output response for neutron energies of 10, 50, 100, 150 and 200 MeV.

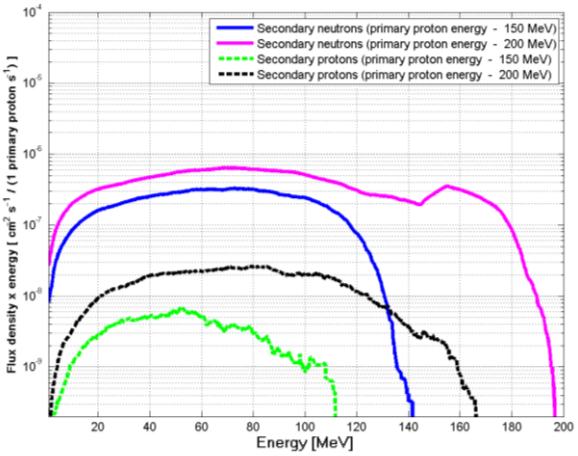

Figure 14. Secondary neutron and proton flux spectra for primary proton energies of 150 and 200 MeV.

8. Conclusion

The neutron measurements performed in this research provided a good test of the newly developed neutron spectrometer. The neutron PH spectra have been collected up to an energy of 200 MeV. The MCNP model of the detector was developed and the simulations of the PH spectra were compared with the measurements. Using the MCNP model we calculated secondary neutron and proton spectra in the vicinity of the irradiated proton therapy phantom. We have calculated the detector response matrix that will be used by a newly developed software module. The module will be able to calculate the neutron flux and ambient dose equivalent H*(10) using the unfolding method.

Acknowledgements: *The presented work has been supported by Ministry of Industry and Trade, within the project TRIO, No. FV20453. Presented results were obtained with a using of the Van de Graaff accelerator laboratory supported by the Ministry of Education, Youth and Sports and from the Proton Therapy Center, Prague.*

References

1. A. Jančář et al., "Pulse-shape discrimination of the new plastic scintillators in neutron–gamma mixed field using fast digitizer card," *Radiation Physics and Chemistry*, vol. 116, pp. 60–64, Nov. 2015. https://doi.org/10.1016/j.radphyschem.2015.05.007
2. F. D. Brooks, "A scintillation counter with neutron and gamma-ray discriminators," *Nucl. Instr. Meth.*, vol. 4, no. 3, pp. 151–163, Apr. 1959. https://doi.org/10.1016/0029-554X(59)90067-9
3. R. A. Winyard, J. E. Lutkin, G. W. McBeth, "Pulse shape discrimination in inorganic and organic scintillators. I," *Nucl. Instr. Meth.*, vol. 95, no. 1, pp. 141–153, Aug. 1971. https://doi.org/10.1016/0029-554X(71)90054-1
4. Z. Matěj at al., "Digital two-parametric processing of the output data from radiation detectors," *Prog. Nucl. Sci. Tech.*, vol. 4, pp. 670–674, Sep. 2014. https://doi.org/10.15669/pnst.4.670
5. G. Dietze, H. Klein, "Gamma-calibration of NE 213 scintillation counters," *Nucl. Instr. Meth. Phys. Res.*, vol. 193, no. 3, pp. 549–556, Mar. 1982. https://doi.org/10.1016/0029-554X(82)90249-X
6. N. Nakao et al., "Measurements of response function of organic liquid scintillator for neutron energy range up to 135 MeV," *Nucl. Instr. Meth. Phys. Res. A*, vol. 362, no. 2–3, pp. 454–465, Aug. 1995. https://doi.org/10.1016/0168-9002(95)00193-X
7. C. J. Werner et al., *MCNP Version 6.2 Release Notes*, Technical Report LA-UR-18-20808, Los Alamos National Laboratory, Los Alamos (NM), USA, 2018. https://doi.org/10.2172/1419730
8. C. J. Werner, Ed., *MCNP® User's Manual*, Technical Report LA-UR-17-29981, Los Alamos National Laboratory, Los Alamos (NM), USA, 2017. Retrieved from: https://mcnp.lanl.gov/pdf_files/TechReport_2017_LANL_LA-UR-17-29981_WernerArmstrongEtAl.pdf Retrieved on: Jun. 15, 2022